Available online at www.sciencedirect.com
ScienceDirect
Journal of the European Ceramic Society 27 (2007) 4215–4218
www.elsevier.com/locate/jeurceramsoc

Lithium mobility in titanium based Nasicon $Li_{1+x}Ti_{2-x}Al_x(PO_4)_3$ and $LiTi_{2-x}Zr_x(PO_4)_3$ materials followed by NMR and impedance spectroscopy

K. Arbi *, J.M. Rojo, J. Sanz

Instituto de Ciencia de Materiales de Madrid (ICMM), Consejo Superior de Investigaciónes Científicas (CSIC), Cantoblanco, 28049 Madrid, Spain

Available online 26 March 2007

Abstract

Titanium-based Nasicon-type compounds with formula $Li_{1+x}Ti_{2-x}Al_x(PO_4)_3$ and $LiTi_{2-x}Zr_x(PO_4)_3$, have been prepared and studied with X-ray Diffraction (XRD), Nuclear Magnetic Resonance (NMR) and Electric Impedance (EI) techniques. From the analysis of the ^7Li and ^{31}P NMR spectra, cation distribution and Li mobility have been deduced. The substitution of Ti^{4+} by a large Zr^{4+} cation expands the unit cell but the grain interior conductivity remains near that of the parent $LiTi_2(PO_4)_3$ compound. However, substitution of Ti^{4+} by a smaller Al^{3+} cation reduces the unit cell dimensions of the Nasicon framework, but enhances about three orders of magnitude the conductivity. In Zr doped samples, the expansion of the unit cell destabilizes Li coordination at M_1 sites; however, in Al doped samples, the increment of Li amount enhances Li–Li repulsions. In both cases, creation of vacancies at M_1 sites increases Li mobility.

Keywords: Powder solid state reaction; X-ray method; NMR spectroscopy; Ionic conductivity; Batteries

1. Introduction

NASICON-type materials with formula $LM_2(PO_4)_3$, $L = Li$, Na and $M = Ge$, Ti, Sn, Hf, Zr, are of increasing interest because of their possible application as solid electrolytes in lithium batteries, sensors and others electrochemical devices.[1] The ideal structure of these compounds is rhombohedral (space group $R\bar{3}c$) but in some of them a low-temperature phase of lower symmetry, has been found.[2–4] In both phases, the framework is built up by $M_2(PO_4)_3$ units in which two MO_6 octahedra and three PO_4 tetrahedra share oxygen atoms. In rhombohedral sodium phases, Na^+ cations are placed at two structural sites: (i) M_1 sites surrounded by six oxygen atoms and located at inversion centers, and (ii) M_2 sites, with an irregular ten-fold oxygen co-ordination and disposed symmetrically around ternary axes. Both sites are arranged in an alternating way along the conducting channels.

In rhombohedral lithium phases, such as $LiGe_2(PO_4)_3$ and $LiTi_2(PO_4)_3$, the preferential occupancy of M_1 sites by lithium has been deduced out from neutron diffraction (ND) experiments.[5] When the size of the tetravalent cation increases (e.g. M = Sn, Hf, Zr), a triclinic phase has been detected. In this phase, Li^+ ions are placed at mid-way $M_{1/2}$ positions between M_1 and M_2 sites in a four-fold oxygen coordination.[2–4] In titanium-based NASICON-type materials, the Li^+ ion conductivity is greatly enhanced when Ti^{4+} is partially replaced by trivalent cations (Al, Ga, Sc, In, Y).[6] The maximum conductivity ($10^{-3}\ \Omega^{-1}\,cm^{-1}$ at 300 K) was achieved at $x \approx 0.3$ in the $Li_{1+x}Ti_{2-x}Al_x(PO_4)_3$ series. In samples with $x > 0.3$, the decrease on the overall conductivity was attributed to the formation of secondary non-conducting phases.[7]

In this work, the structure of $Li_{1+x}Ti_{2-x}Al_x(PO_4)_3$ ($0 \le x \le 0.7$) and $LiTi_{2-x}Zr_x(PO_4)_3$ ($0 \le x < 2$) series has been assessed by X-ray diffraction technique. Distribution of octahedral cations has been followed by ^{31}P MAS-NMR spectroscopy sites and mobility of lithium have been investigated by ^7Li MAS-NMR technique. Electric impedance technique has been used to analyze Li conductivity in prepared samples.

2. Experimental procedure

$Li_{1+x}Ti_{2-x}Al_x(PO_4)_3$ and $LiTi_{2-x}Zr_x(PO_4)_3$ series, were prepared following the method described elsewhere.[7] X-ray

* Corresponding author.
E-mail addresses: kamel.arbi@icmm.csic.es, Kamel@ceu.es (K. Arbi).

0955-2219/$ – see front matter © 2007 Elsevier Ltd. All rights reserved.
doi:10.1016/j.jeurceramsoc.2007.02.118

diffraction patterns were recorded at room temperature with Cu Kα radiation (λ = 1.5405981 Å) in a PW-1710 Phillips diffractometer. Data were taken in the $10 \leq 2\theta \leq 70^\circ$ range with 0.02° per step, counting for 0.5 s at each step.

Impedance measurements were carried out on cylindrical pellets of 13 mm diameter and approximately 1.4 mm thick. Pellets were first compacted by cold pressing at 3 MPa, then sintered at 950–1000 °C for 24 h. For electric measurements, platinum electrodes were deposited by sputtering on the two faces of the pellet. The impedance measurements performed over the frequency range 10^{-1} to 1.8×10^9 Hz at increasing temperatures (150–500 K) allowed us to separate grain interior and grain boundary contributions. From 10^{-1} to 10^6 Hz a Solartron SI 1260 was used; however, for the high frequency range (10^6–1.8×10^9 Hz) an HP 4291A rf impedance analyzer was taken. In this case, the sample was located at the end of a coaxial line and the impedance was deduced from the analysis of the complex reflection factor. In both cases, the sample temperature was measured with accuracies better than ±1 K.

^{31}P and ^{7}Li MAS-NMR spectra were recorded at room temperature in a MSL-400 Bruker spectrometer (9.4 T). The frequencies used for ^{31}P an ^{7}Li signals were 161.97 and 155.50 MHz, respectively. Samples were spun at 4 kHz during signal recording. Spectra were obtained after single pulse irradiation with a recycling time of 10 s. In the temperature range 100–450 K, quadrupole interactions deduced from ^{7}Li spectra remains small ($C_Q < 180$ kHz), making the irradiation of the central and satellite transitions non-selective. The number of scans was in the range of 100–800. ^{7}Li and ^{31}P chemical shift values were given relative to 1 M LiCl and 85% H_3PO_4 aqueous solutions. The fitting of the NMR spectra was done with the Bruker WINFIT software package.[8] This program allows the position, line width and intensity of components to be determined; however, quadrupole C_Q and η values have to be deduced with a trial and error procedure.

3. Results and discussions

3.1. Cation distribution

XRD patterns of $Li_{1+x}Ti_{2-x}Al_x(PO_4)_3$ and $LiTi_{2-x}Zr_x(PO_4)_3$ samples, recorded at room temperature, display peaks of the rhombohedral ($R\bar{3}c$ space group) phase. The substitution of Ti

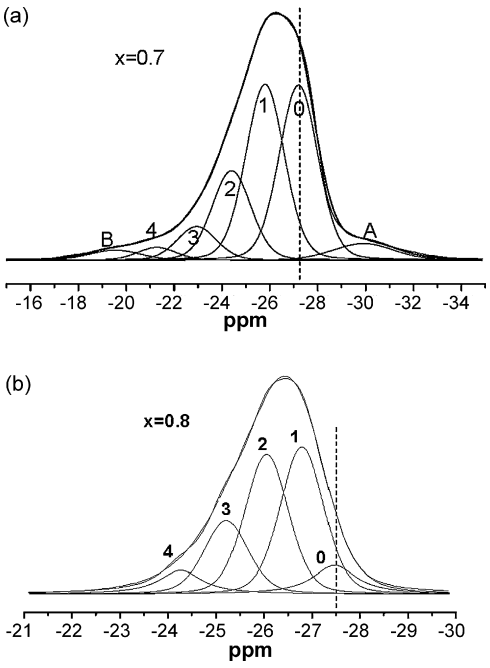

Fig. 1. ^{31}P MAS-NMR spectra of (a) $Li_{1+x}Ti_{2-x}Al_x(PO_4)_3$ and (b) $LiTi_{2-x}Zr_x(PO_4)_3$ series at indicated nominal compositions. The vertical line corresponds to the line position of undoped sample.

(0.60 Å)[9] by a larger Zr^{4+} cation ($r = 0.72$ Å) produces the progressive enlargement of the rhombohedral unit cell. However, the progressive substitution for Ti^{4+} by Al^{3+} (0.53 Å) reduces slightly the parameters of the hexagonal unit cell. The decrease observed on a and c parameters is lower in samples with $x > 0.3$, suggesting that only part of Al was incorporated into the Nasicon structure (Table 1).

In $LiTi_2(PO_4)_3$, the ^{31}P MAS-NMR spectrum is formed by a single line at −27.5 ppm. In Ti-based series, the substitution of Ti by Zr or Al produces the broadening and the shift of ^{31}P NMR line towards more positive values, indicating the creation of new P environments. In ^{31}P NMR spectra (Fig. 1), the shift produced by substitution of Ti by Al (or Zr) was assumed to be additive, allowing the detection of components associated with $P(OTi)_4$, $P(OTi)_3(OM)_1$, $P(OTi)_2(OM)_2$, $P(OTi)_1(OM)_3$ and $P(OM)_4$ environments (lines labeled 0, 1, 2, 3 and 4). The quantitative analysis of the ^{31}P NMR spectra allowed an estimation of the Al (or Zr) content in NASICON phases. The Al/Ti

Table 1
Hexagonal unit cell parameters and quadrupole C_Q constants of $Li_{1+x}Ti_{2-x}Al_x(PO_4)_3$ and $LiTi_{2-x}Zr_x(PO_4)_3$ series

$Li_{1+x}Ti_{2-x}Al_x(PO_4)_3$				$LiTi_{2-x}Zr_x(PO_4)_3$			
x	a (Å)	c (Å)	C_Q (kHz)	x	a (Å)	c (Å)	C_Q (kHz)
0.1	8.508(1)	20.79(2)	44 ± 2	0	8.511(1)	20.84(2)	44 ± 2
0.2	8.501(1)	20.77(2)	44.1 ± 2	0.4	8.566(1)	21.07(2)	50 ± 2
0.3	8.497(1)	20.74(2)	44.2 ± 2	0.63	8.605(1)	21.21(2)	73 ± 2
0.4	8.489(1)	20.73(2)	44.6 ± 2	1	8.672(1)	21.46(2)	88 ± 3
0.5	8.485(1)	20.72(2)	46.1 ± 2	1.5	8.764(1)	21.77(2)	100 ± 3
0.7	8.480(1)	20.70(2)	47.8 ± 2	2	8.847(1)	22.24(2)	120 ± 4

ratio (or Zr/Ti) was estimated with the expression:[10]

$$\frac{Al^{3+}}{Ti^{4+}} = \frac{4I_4 + 3I_3 + 2I_2 + I_1}{I_3 + 2I_2 + 3I_1 + 4I_0} = \frac{x}{2-x}$$

where I_n ($n = 0, 1, 2, 3, 4$) stands for the intensity of bands associated with $(4-n)$Ti (n)Al environments.

From the analysis of ^{31}P MAS-NMR spectra, it has been deduced that most part of Zr was incorporated in the Nasicon structure, but that the substitution of Ti by Al at octahedral sites remains always partial. In agreement with unit cell data of the $Li_{1+x}Ti_{2-x}Al_x(PO_4)_3$ series, a significant part of Al must be placed outside of the Nasicon structure. In samples with $x > 0.3$, a new NMR line was detected at −30 ppm in ^{31}P MAS-NMR spectra (line A of Fig. 1a), that increases with the Al content, indicating in agreement with XRD data, the formation of the $AlPO_4$ phosphate. Moreover, XRD patterns of these samples (not shown) showed the presence of another crystalline phase, identified as $Li_4P_2O_7$. The formation of this phase produced the detection of new components at ∼0 ppm in the ^{7}Li MAS-NMR spectra (not shown) and at −19 ppm in the ^{31}P MAS-NMR spectra (line B of Fig. 1a).

3.2. Li mobility

In $LiTi_{2-x}Zr_x(PO_4)_3$ series, the substitution of Ti by Zr expands the unit cell, increasing triangular windows that relate M_1 and $M_{1/2}$ sites. This fact favors lithium mobility, decreasing activation energy values along the series. In parallel with this observation, the quadrupole C_Q constant deduced from ^{7}Li NMR spectra increase from 40 to 120 kHz, indicating that Li ions occupy not only M_1 sites ($C_Q = 40$ kHz) sites but also $M_{1/2}$ sites ($C_Q = 180$ kHz). The increment of lithium mobility favors fast exchange processes between M_1 and $M_{1/2}$ sites, giving intermediate C_Q values (Fig. 2a). In samples with $x > 1.5$, quadrupole constants measured at room temperature are near those measured in the rhombohedral $LiZr_2(PO_4)_3$ phase, obtained by heating the triclinic phase above the phase transition temperature[3] (Fig. 2b). The stabilization of the rhombohedral phase in Zr doped samples eliminates problems derived from stresses produced at the triclinic–rhombohedral transition and enlarges the electrochemical window (lower reducibility of Zr). In this series, activation energy decreases from 0.45 to 0.3 eV as the Zr content increases; but, ionic conductivity does not increase appreciably with respect to that measured in $LiTi_2(PO_4)_3$ (Fig. 3).

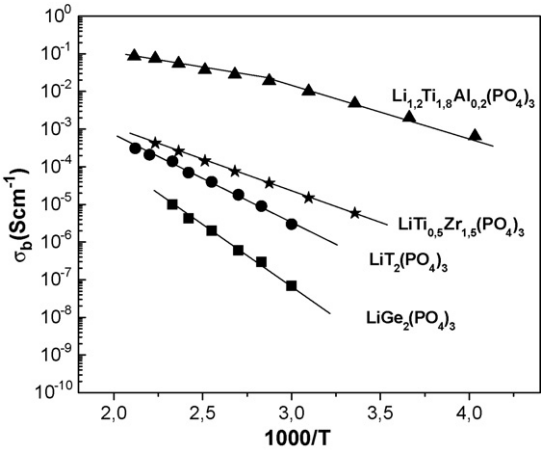

Fig. 3. Grain interior dc conductivity vs. reciprocal temperature in lithium conductors with Nasicon structure.

In $Li_{1+x}Ti_{2-x}Al_x(PO_4)_3$ series, the incorporation of an additional amount of Li increases Li–Li repulsions and destabilizes the occupation of M_1 sites. This makes that Li ions occupy besides M_1 sites other more distorted $M_{1/2}$ sites in conducting paths. According to this study, exchange processes between M_1 and $M_{1/2}$ sites explains the small increment detected on the quadrupole constant C_Q at increasing temperatures (Table 1). As the Li content increases, the ionic conductivity increases to reach a maximum at $x_{Al} = 0.2$ ($\sigma_b \approx 5 \times 10^{-3}$ S cm^{-1} at 298 K) and then decreases slightly.[7] In this series, activation energy decreases from 0.45 to 0.29 eV as the Al content increases.

In the best ion conductor of the $Li_{1+x}Ti_{2-x}Al_x(PO_4)_3$ series ($x = 0.2$), a non-Arrhenius behavior was observed on the grain interior dc-conductivity[11,12] and the activation energy, E_m, decreased from 0.29 eV for low temperatures regime to 0.18 eV for the high temperature regime (Fig. 3). The latter value coincides with microscopic activation energy deduced from NMR

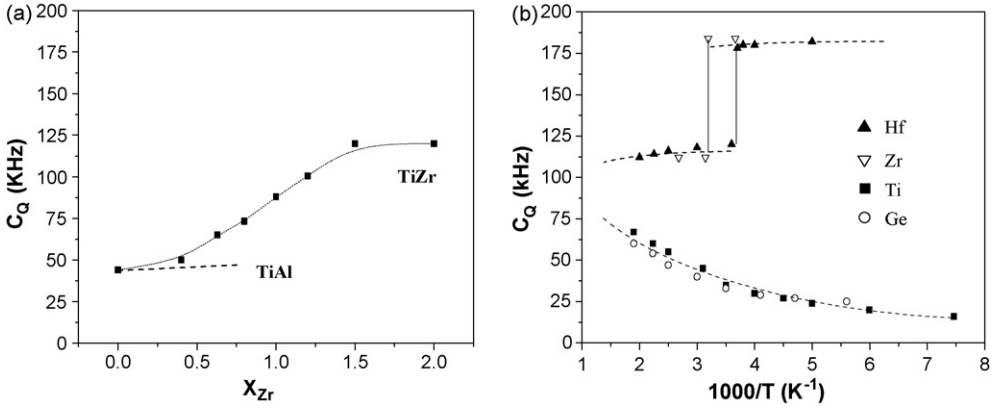

Fig. 2. (a) Dependence of the quadrupole C_Q constant on the composition of the $LiTi_{2-x}Zr_x(PO_4)_3$ and $Li_{1+x}Ti_{2-x}Al_x(PO_4)_3$ series. (b) Temperature dependence of quadrupole C_Q constants, deduced from ^{7}Li NMR spectra of $LiR_2(PO_4)_3$ series, R = Ge, Ti, Zr and Hf.

data, $E_m = 0.20$ eV.[11] This observation was explained by assuming the presence of correlation effects in the Li motion, that disappear as temperature increases[11].

4. Conclusions

Cation solution has been analysed in rhombohedral $Li_{1+x}Ti_{2-x}Al_x(PO_4)_3$ and $LiTi_{2-x}Zr_x$ $(PO_4)_3$ series with NMR and XRD techniques. In the first case, the solution range was partial ($0 < x < 0.7$); but in the second case, the solution range was almost complete ($0 < x < 1.8$). In the case of $LiTi_{2-x}Zr_x(PO_4)_3$ series, the substitution of Ti by Zr enlarges the unit cell and produces the delocalization of lithium on M_1 and $M_{1/2}$ sites. The stabilization of the rhombohedral phase in Zr doped samples eliminates problems derived from stresses produced at the triclinic-rhombohedral transition and enlarges the electrochemical window of samples. However, conductivity values deduced in this series remains near those measured in the parent $LiTi_2(PO_4)_3$.

Substitution of Ti^{4+} by Al^{3+} in $Li_{1+x}Ti_{2-x}Al_x(PO_4)_3$ series reduces unit cell dimensions but increases Li conductivity three orders of magnitude with respect to that of $LiTi_2(PO_4)_3$ sample. For $x_{Al} = 0.2$, activation energy decreases from 0.29 to 0.18 as temperature increases, producing a clear deviation of conductivity from the Arrhenius behaviour. The improvement of conductivity has been ascribed to the progressive cancellation of correlation effects, produced by the creation of vacant M_1 sites in the Nasicon structure. For $x > 0.3$ samples, ionic conductivity decreases as a consequence the formation of secondary $AlPO_4$ and $Li_4P_2O_7$ phases at the surface of Nasicon phase particles.

Acknowledgements

This work was supported by the Spanish CICyT Agency (projects MAT2001-3713 and MAT2004-3070) and the regional Government of Madrid (project S-0505/PPQ-0358). K. Arbi thanks Spanish Ministry of Science and Technology for the financial support.

References

1. Goudenough, J. B., Hong, H. Y.-P. and Kafalas, J. A., Fast Na^+ ion transport in skeleton structures. *Mater. Res. Bull.*, 1976, **11**, 203–220.
2. Morin, E., Angenault, J., Couturier, J. C., Quarton, M., He, H. and Klinowski, J., Phase transition and crystal structures of $LiSn_2(PO_4)_3$. *Eur. J. Solid State Inorg. Chem.*, 1997, **34**, 947–958.
3. Catti, M., Stramare, S. and Ibberson, R., Lithium location in NASICON-type Li^+ conductors by neutron diffraction. I. Triclinic α'-$LiZr_2(PO_4)_3$. *Solid State Ionics*, 1999, **123**, 173–180.
4. Losilla, E. R., Aranda, M. A. G., Martinez-Lara, M. and Bruque, S., Reversible triclinic–rhombohedral phase transition in $LiHf_2(PO_4)_3$: crystal structures from neutron powder diffraction. *Chem. Mater.*, 1997, **9**, 1678–1685.
5. Alami, M., Brochu, R., Soubeyroux, J. L., Gravereau, P., Leflem, G. and Hagenmuller, P., Structure and thermal-expansion of $LiGe_2(PO_4)_3$. *J. Solid State Chem.*, 1991, **90**, 185–193.
6. Aono, H., Sugimoto, E., Sadaoka, Y., Imanaka, N. and Adachi, G.-Y., Ionic-conductivity of solid electrolytes based on lithium titanium phosphate. *J. Electrochem. Soc.*, 1990, **137**, 1023–1027.
7. Arbi, K., Mandal, S., Rojo, J. M. and Sanz, J., Dependence of ionic conductivity on composition of fast ionic conductors $Li_{1+x}Ti_{2-x}Al_x$ $(PO_4)_3$. $0 \leq x \leq 0.7$. A parallel NMR and electric impedance study. *Chem. Mater.*, 2002, **14**, 1091–1097.
8. Massiot, D., *WINFIT; Bruker-Franzen Analytik GmbH*. Bremen, Germany, 1993.
9. Shannon, R. D., Revised effective ionic-radii and systematic studies of interatomic distances in halides and chalcogenides. *Acta Cryst.*, 1976, **A32**, 751–767.
10. Losilla, E. R., Aranda, M. A. G., Bruque, S., París, M. A., Sanz, J., Campo, J. and West, A. R., Sodium mobility in the NASICON series $Na_{1+x}Zr_{2-x}In_x(PO_4)_3$. *Chem. Mater.*, 2000, **12**, 2134–2142.
11. Arbi, K., Tabellout, M., Lazarraga, M. G., Rojo, J. M. and Sanz, J., Non-Arrhenius conductivity in the fast lithium conductor $Li_{1.2}Ti_{1.8}Al_{0.2}(PO_4)_3$: a ^7Li NMR and electric impedance study. *Phys. Rev. B*, 2005, **72**, 094302.
12. Robertson, A. D., West, A. R. and Ritchie, A. G., Review of crystalline lithium-ion conductors suitable for high temperature battery applications. *Solid State Ionics*, 1997, **104**, 1–11.